Journal Pre-proof

Analysis of source regions and transport pathways of sub-micron aerosol components in Europe

Michelle Y. Schneider, Jianhui Jiang, Ying Chen, Wenche Aas, Samira Atabakhsh, Minna Aurela, Claudio Belis, Aikaterini Bougiatioti, Michael Bressi, Francesco Canonaco, Benjamin Chazeau, Hasna Chebaicheb, Mikael Ehn, Konstantinos Eleftheriadis, Olivier Favez, Harald Flentje, Anna Font, Evelyn Freney, Stefania Gilardoni, Maria I. Gini, David C. Green, Liine Heikkinen, Hannes Keernik, Radek Lhotka, Chunshui Lin, Marek Maasikmets, Nicolas Marchand, María Cruz Minguillón, Jaroslaw Necki, Jurgita Ovadnevaite, Marco Paglione, Julija Pauraite, Jean-Eudes Petit, Michael Pikridas, Stephen Platt, Petra Pokorná, Vanes Poluzzi, Laurent Poulain, Véronique Riffault, Matteo Rinaldi, Jean Sciare, Yulia Sosedova, Iasonas Stavroulas, Hilkka Timonen, Anna Tobler, Jeni Vasilescu, Marta Via, Petr Vodička, Yunjiang Zhang, Olga Zografou, Kaspar Rudolf Dällenbach, Abhishek Kumar Upadhyay, Gang I. Chen, Manousos-Ioannis Manousakas, Imad El Haddad, André S.H. Prévôt

PII: S0269-7491(25)01484-8

DOI: https://doi.org/10.1016/j.envpol.2025.127110

Reference: ENPO 127110

To appear in: *Environmental Pollution*

Received Date: 11 January 2025

Revised Date: 25 August 2025

Accepted Date: 10 September 2025

Please cite this article as: Schneider, M.Y., Jiang, J., Chen, Y., Aas, W., Atabakhsh, S., Aurela, M., Belis, C., Bougiatioti, A., Bressi, M., Canonaco, F., Chazeau, B., Chebaicheb, H., Ehn, M., Eleftheriadis, K., Favez, O., Flentje, H., Font, A., Freney, E., Gilardoni, S., Gini, M.I., Green, D.C., Heikkinen, L., Keernik, H., Lhotka, R., Lin, C., Maasikmets, M., Marchand, N., Minguillón, M.C., Necki, J., Ovadnevaite, J., Paglione, M., Pauraite, J., Petit, J.-E., Pikridas, M., Platt, S., Pokorná, P., Poluzzi, V., Poulain, L., Riffault, V., Rinaldi, M., Sciare, J., Sosedova, Y., Stavroulas, I., Timonen, H., Tobler, A., Vasilescu, J., Via, M., Vodička, P., Zhang, Y., Zografou, O., Dällenbach, K.R., Upadhyay, A.K., Chen, G.I., Manousakas, M.-I., El Haddad, I., Prévôt, A.S.H., Analysis of source regions and transport pathways

of sub-micron aerosol components in Europe, *Environmental Pollution*, https://doi.org/10.1016/j.envpol.2025.127110.

Analysis of source regions and transport pathways of sub-micron aerosol components in Europe

Michelle Y. Schneider[1,2], Jianhui Jiang[3], Ying Chen[4], Wenche Aas[5], Samira Atabakhsh[6], Minna Aurela[7], Claudio Belis[8], Aikaterini Bougiatioti[9], Michael Bressi[8], Francesco Canonaco[10], Benjamin Chazeau[1,11], Hasna Chebaicheb[12,13,14], Mikael Ehn[15], Konstantinos Eleftheriadis[16], Olivier Favez[13,14], Harald Flentje[17], Anna Font[2,a], Evelyn Freney[18], Stefania Gilardoni[19], Maria I. Gini[16], David C. Green[2], Liine Heikkinen[15,20,21], Hannes Keernik[22], Radek Lhotka[23], Chunshui Lin[24], Marek Maasikmets[22], Nicolas Marchand[11], María Cruz Minguillón[25], Jaroslaw Necki[26], Jurgita Ovadnevaite[24], Marco Paglione[27], Julija Pauraite[28], Jean-Eudes Petit[29], Michael Pikridas[30], Stephen Platt[5], Petra Pokorná[23], Vanes Poluzzi[31], Laurent Poulain[6], Véronique Riffault[12,14], Matteo Rinaldi[27], Jean Sciare[30], Yulia Sosedova[10], Iasonas Stavroulas[9], Hilkka Timonen[7], Anna Tobler[10], Jeni Vasilescu[32], Marta Via[25,b], Petr Vodička[23], Yunjiang Zhang[33], Olga Zografou[16], Kaspar Rudolf Dällenbach[1], Abhishek Kumar Upadhyay[1], Gang I. Chen[2*], Manousos-Ioannis Manousakas[1,c*], Imad El Haddad[1], André S.H. Prévôt[1]

[1]PSI Center for Energy and Environmental Sciences, 5232, Villigen, Switzerland
[2]MRC Centre for Environment and Health, Environmental Research Group, Imperial College London, W12 0BZ, London, United Kingdom
[3]Shanghai Key Lab for Urban Ecological Processes and Eco-Restoration, 200241, Shanghai, China
[4]College of Life and Environmental Sciences, University of Birmingham, B15 2TT, Birmingham, United Kingdom
[5]NILU, Kjeller, 2007, Norway
[6]Leibniz Institute for Tropospheric Research (TROPOS), 04 318, Leipzig, Germany
[7]Atmospheric Composition Research, Finnish Meteorological Institute, 00101, Helsinki, Finland
[8]European Commission - Joint Research Centre, Unit Clean Air and Climate, 21027, Ispra, Italy
[9]Institute for Environmental Research and Sustainable Development, National Observatory of Athens, 15236, Athens, Greece
[10]Datalystica Ltd., Parkstrasse 1, 5234, Villigen, Switzerland
[11]Aix Marseille Univ, LCE, Marseille, France
[12] IMT Nord Europe, Institut Mines-Télécom, Université de Lille, Centre for Energy and Environment, 59000, Lille, France
[13]Institut National de l'Environnement Industriel et des Risques (INERIS), 60550, Verneuil-en-Halatte, France
[14]Laboratoire Central de Surveillance de la Qualité de l'Air (LCSQA), 60550, Verneuil-en-Halatte, France
[15]Institute for Atmospheric and Earth System Research/Physics , Faculty of Science, University of Helsinki, 00014, Helsinki, Finland
[16]ENRACT, Institute of Nuclear and Radiological Science & Technology, Energy & Safety, NCSR Demokritos, 15310, Athens, Greece
[17]German Meteorological Service (DWD), 82383, Observatory Hohenpeissenberg, Germany
[18]Laboratoire de Météorologie Physique, UMR6016, Université Clermont Auvergne-CNRS, 63170, Aubière, France
[19]National Research Council, Institute of Polar Sciences (CNR-ISP), 40129, Bologna, Italy
[20]Department of Environmental Science, Stockholm University, 114 18, Stockholm, Sweden
[21]Bolin Centre for Climate Research, 114 18, Stockholm, Sweden
[22]Air Quality and Climate Department, Estonian Environmental Research Centre (EERC), Marja 4D, Tallinn, Estonia
[23]Institute of Chemical Process Fundamentals, Czech Academy of Sciences, Rozvojová 1, 16500 Prague 6, Czech Republic

[24]*School of Natural Sciences, Physics, University of Galway, Centre for Climate and Air Pollution Studies, Ryan Institute, H91 CF50, Galway, Ireland*
[25]*Institute of Environmental Assessment and Water Research (IDAEA), Spanish National Research Council (CSIC), 08034, Barcelona, Spain*
[26]*AGH University of Krakow, Faculty of Physics and Applied Computer Science, 30-059, Krakow, Poland*
[27]*Italian National Research Council - Institute of Atmospheric Sciences and Climate (CNR-ISAC), 40129, Bologna, Italy*
[28]*SRI Center for Physical Sciences and Technology (FTMC), 10257, Vilnius, Lithuania*
[29]*Laboratoire des Sciences du Climat et de l'Environnement (LSCE), 91190, Gif-sur-Yvette, France*
[30]*Climate and Atmosphere Research Center (CARE-C), The Cyprus Institute, 2121, Nicosia, Cyprus*
[31]*Arpae Emilia-Romagna, Centro Tematico Regionale Qualità dell'Aria, 40139, Bologna, Italy*
[32]*National Institute of Research and Development for Optoelectronics, 077125, Magurele, Romania*
[33]*Collaborative Innovation Center of Atmospheric Environment and Equipment Technology, Jiangsu Key Laboratory of Atmospheric Environment Monitoring and Pollution Control, Joint International Research Laboratory of Climate and Environment Change, School of Environmental Science and Engineering, Nanjing University of Information Science and Technology, 210044, Nanjing, China*

[a]*Now at: IMT Nord Europe, Institut Mines-Télécom, Université de Lille, Centre for Energy and Environment 59000, Lille, France*
[b]*Now at: Now at: Center for Atmospheric Research, University of Nova Gorica, 5270 Ajdovščina, Slovenia*
[c]*Now at: ENRACT, Institute of Nuclear and Radiological Science & Technology, Energy & Safety, NCSR Demokritos, 15310, Athens, Greece*

∗Corresponding authors: Email address: gang.chen@imperial.ac.uk (Gang I. Chen), manousos.manousakas@psi.ch (Manousos-Ioannis Manousakas)

Abstract

It is important to study aerosols and their origins, as they pose various negative health and environmental impacts. In this study, we combined year-long datasets from 15 different countries with Trajectory Statistical Methods (TSMs) on such a comprehensive scale for the first time. We found possible source regions and seasonal variations of various particulate matter (PM) components, including total organic aerosol (OA), biomass burning OA (BBOA), oxygenated OA (OOA), ammonium (NH_4), nitrate (NO_3), and sulphate (SO_4) in Europe. We found that for all of the studied components, Eastern Europe was among the highest contributors. For NO_3, other important source regions were northern France and the Benelux, while for SO_4, there were significant contributions from the Mediterranean region. We also compared our measurement-based model with simulated concentrations of an atmospheric chemistry transport model (CAMx). We observed a satisfactory agreement in regions where we had sufficient coverage with air pollution monitoring stations. The main deviations for OA were found around the Po Valley, where CAMx consistently estimated higher concentrations, while the TSM analysis did not highlight it as a hot spot because long-term monitoring data sets in this region are lacking. CAMx also underestimated the concentrations around Poland, mainly from residential burning. Our results provide opportunities to refine European emission inventories and deliver valuable information on long-range transported air pollutants. It suggests that policies mitigating air pollution in Eastern Europe and the Benelux could help improve overall air quality in entire Europe more efficiently.

1 Introduction

Particulate matter (PM) remains a persistent environmental challenge, with adverse effects on human health, ecological systems, and global climate (Harrison & Yin, 2000). PM varies in size and composition and is emitted from a wide range of sources, encompassing both natural and human emissions. Among the primary sources of PM are transportation, biomass burning, dust resuspension, industrial processes, and agricultural activities. The impacts of PM on human health are profound and diverse. Inhalation of PM can lead to respiratory problems such as asthma, bronchitis, and other respiratory infections (Samoli et al., 2016). Fine particulate matter, known as $PM_{2.5}$ (particles with aerodynamic diameters of 2.5 micrometres or smaller), can penetrate deep into the lungs and even enter the bloodstream, increasing the risk of cardiovascular diseases, strokes, cancers, and other systemic health issues (Mitsakou et al., 2007).

Particulate matter consists of both organic and inorganic components. Examples of the latter are sulphate, nitrate, chloride, ammonium, and black carbon. The sources and formation processes of these inorganic components are relatively understood, while the other part of PM, organic aerosols (OA), consists of thousands of compounds; therefore, their formation processes and sources remain challenging to deconvolve. Previous measurements across the world suggested that OA can dominate the overall PM mass and consist of 20–90% of the total PM mass (Chen et al., 2022; Crippa et al., 2014; Jimenez et al., 2009). Recent studies have reported an overview of OA sources in Europe by employing advanced source apportionment techniques (Calvin et al., 2023; G. Chen et al., 2022).

While local sources undoubtedly play a significant role in aerosol pollution, it is crucial not to overlook the substantial impact of transboundary transport. PM can travel vast distances, extending far beyond its original emission point and affecting regions remote from its sources. To better grasp the complex interactions between aerosols and long-range transport, researchers have increasingly turned to trajectory statistical methods (TSMs) (Salvador et al., 2008). These analytical techniques leverage air mass backward trajectories, which trace the path of air masses from receptor locations back to their source regions, and PM concentration data collected at various receptors (Salvador et al., 2010). TSMs do not account for factors like atmospheric dispersion, chemical conversion, or dry and wet deposition through the Hybrid Single-Particle Lagrangian Integrated Trajectory model (HYSPLIT) (NOAA, accessed 1.11.25), developed by NOAA's Air Resources Laboratory. However, they offer simplicity and effectiveness in application. TSMs can assist in pinpointing relevant source regions and distinguishing the airflow patterns associated with the transport of regional and large-scale air pollution. By examining the relationship between air mass trajectories and PM concentrations, TSMs enable the identification of potential emission hotspots, the characterisation of pollutant transport pathways, and the assessment of the efficacy of regional air quality management strategies. Utilising TSMs with a large number of trajectories can notably diminish trajectory uncertainty, which arises from interpolation and truncation processes, low temporal or spatial resolution of wind data, or inadequate selection of starting heights (Lupu & Maenhaut, 2002).

Previous studies have highlighted the potential of incorporating multiple receptors in TSMs to enhance accuracy (Hsu et al., 2003; Lee & Ashbaugh, 2007). In this study, we leverage comprehensive datasets utilised in harmonised OA source apportionment across Europe to identify

potential source hotspots in the region using TSMs. This has not been done previously on this scale and with this level of high-quality source apportionment data from high-time resolution measurements (30 min to 4 hours). By integrating all datasets, trajectories converge at various receptor sites, facilitating a more robust analysis (Stohl, 1996). This convergence, together with variations in concentrations at each site, amplify the redistribution process, thereby improving efficacy. The findings from TSM-based investigations are invaluable for policymakers, environmental agencies, and public health authorities aiming to devise targeted interventions to mitigate the impacts of transboundary aerosol pollution.

2 Methodology

In this study, we used the chemical composition data and the source apportionment results of 22 air quality observational sites from 15 different countries over Europe, published in (Chen et al., 2022). The source apportionment results were retrieved through Positive Matrix Factorization (PMF) analysis by following the harmonized protocol in Chen et al. (2022). In addition, 5 sites in Italy were included, some of whose observational results have been published previously in Paglione et al. (2020). An overview of the countries and the measurement periods can be found in Figure 1. Measurement devices include the Aerodyne Aerosol Mass Spectrometer (AMS) and the Aerosol Chemical Speciation Monitor (ACSM), which both deliver real-time mass concentrations of aerosol species (i.e., organic, nitrate, sulphate, ammonium, and chloride). In particular, data from 18 Q-ACSM (quadrupole ACSM (Ng et al., 2011)), 3 ToF-ACSM (time-of-flight ACSM (Fröhlich et al., 2013)), 1 C-ToF-AMS (compact time-of-flight AMS (Drewnick et al., 2005)), and

2 HR-ToF-AMS (High-Resolution ToF-AMS (Paglione et al., 2020)) were used in this study. All ACSM data used here comply with the Standard Operation Procedures (SOP) (COST COLOSSAL Q-ACSM SOP 2021; ToF-ACSM SOP, 2022) of the instruments as best as possible. Intercomparisons of the ACSM instruments have been performed regularly (Crenn et al., 2015; Freney et al., 2019; Fröhlich et al., 2015; Mărmureanu et al., 2025), thus systematic uncertainties of the instruments have been minimized. In addition, the procedures to calibrate the different versions of ACSM and AMS are essentially the same to ensure consistency in accuracy across measurement sites.

The measurements of the concentrations were averaged every 12 hours (at 12 a.m. and 12 p.m.). These averaged values were used in TSMs analysis by combining them with trajectory endpoints using an R script. The script can be found in the supplementary material. A statistical analysis (Concentration Weighted Trajectory, CWTs) was done using the **openair** R package (Carslaw, 2019), an open-source tool for analysing air pollution data. The R script for the plotting can be found in the supplementary material, and the results are shown in section 3.

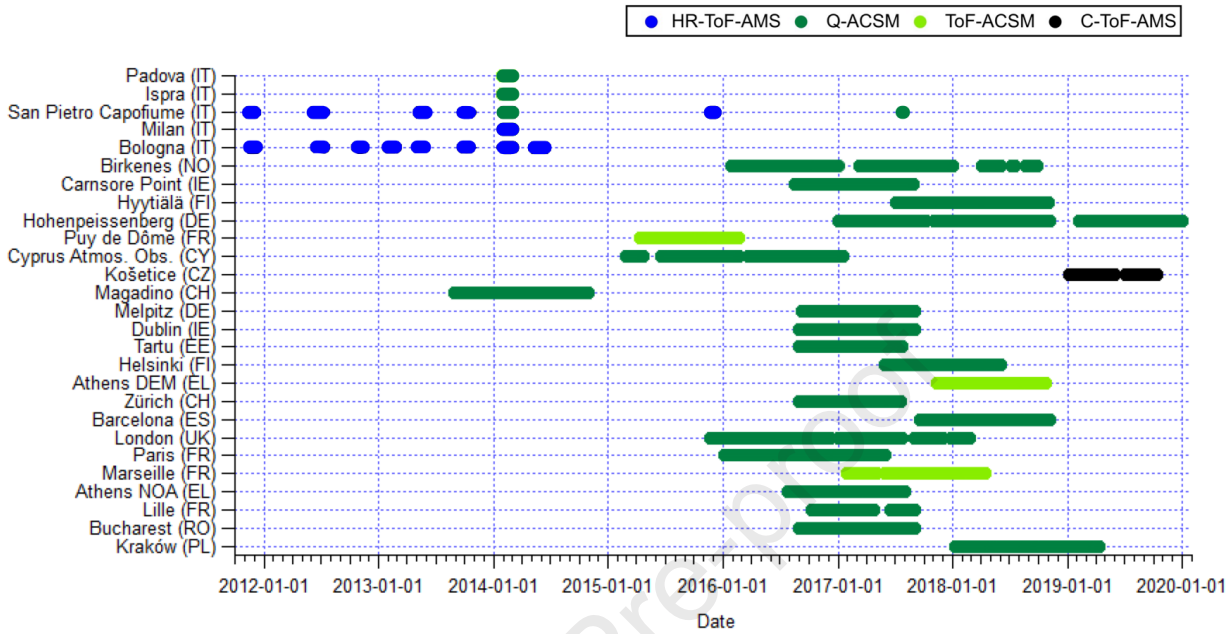

Fig. 1. The contributing countries and the measurement periods considered in this experiment. 24 ACSM measurements and 3 AMS measurements were used in this study (Chen et al., 2022; Paglione et al., 2020).

We chose to focus on specific PM factors based on their universality, i.e., their presence in most of the stations, as well as their relative importance, based on the results from Chen et al. (2022). We studied two organic PM factors: biomass burning OA (BBOA) and oxygenated OA (OOA), as well as total organics, i.e., the sum of all OA factors. BBOA originates mainly from residential heating activities, therefore it is more regional and could be more prevalent in rural areas. OOA is an important factor, as it makes up 70% of total OA. Rapid oxidation of primary emissions (e.g., BBOA, HOA, COA, biogenic) can be a considerable pathway of OOA formation. Consequently, biogenic OOA is more prevalent in warmer seasons, while anthropogenic OOA has larger contributions in colder seasons. In addition, OOA is expected to be transported over long distances. Other organic components resolved by Chen et al. (2022), such as traffic OA or cooking OA, were not considered, as they only exist in specific urban environments. Even more site-specific factors,

such as cigarette smoke and ship industry OA, were also not considered for the same reasoning. Additionally, we also considered three inorganic PM components: ammonium (NH_4), nitrate (NO_3), and sulphate (SO_4). NH_4 contributes on average 10% of overall sub-micron aerosol. In Europe, ammonium emissions are dominated by agriculture, with some contribution from traffic exhausts (Liu et al., 2024). NO_3 has a similar overall PM contribution but shows a higher variability than NH_4, as it can make up to 30% of total aerosol. NO_3 comes from the oxidation of NO_x, which in Europe is mostly emitted from traffic and industry. SO_4 is the highest inorganic sub-micron aerosol contributor, on average 16%. Sulphate originates from the oxidation of SO_2, mainly emitted from heavy fuel oil and coal combustion (Bressi et al., 2021).

2.1 Back-trajectory analysis

The backward trajectories were modelled using HYSPLIT. It has been widely used in many previous studies to successfully investigate the impacts of atmospheric transport and dispersion all over the world (Chen et al., 2021; Escudero et al., 2011; Stein et al., 2015). For the input meteorological data, we used the GDAS (Global Data Assimilation System) global archive from 2006–present with 1-degree resolution, provided by the National Weather Service's National Centres for Environmental Prediction (NCEP) (GDAS, accessed 1.11.2025). We used each of the 27 measurement stations as end points and modelled one 72-hour back-trajectory every 12 hours (at 12 a.m. and 12 p.m. UTC) for the periods where the ACSM/AMS data were available, with consideration of the computational capacity. The height of the trajectories arriving at the end points was set to 200 metres above ground, and points in the trajectories reaching over 1500 metres above ground were filtered out.

Generally, trajectory positional uncertainties range from ±15% to ±30% of the path length, depending on atmospheric conditions and data resolution (Draxler, 1999; Stohl, 1998). For HYSPLIT, the error of individual trajectories is typically around 1-3 degrees of latitude/longitude at mid-latitudes. By aggregating a large number of trajectories in TSMs, the influence of the individual errors decreases, as they are typically normally distributed and tend to cancel each other out. TSMs are able to accurately predict broad areas of pollution sources, even if the endpoints of the trajectories are subject to errors: Repeatedly elevated pollution levels associated with a specific region will still be captured in the statistical output. While interpreting the results, it is important to note that TSMs are useful to determine broad source regions, rather than point sources (Stohl, 1996).

2.2 Concentration weighted trajectory

The **openair** package provides two kinds of statistical methods to identify possible source locations by using back-trajectories: the Potential Source Contribution Function (PSCF) and the Concentration Weighted Trajectory (CWT). Both methods divide the map into grid cells (i, j) and can be easily applicable to multiple receptors. The PSCF method takes the number of times a source concentration was high when the trajectories passed through the cell (i, j), and divides it by the number of times a trajectory passed through the cell (i, j). The CWT, on the other hand, calculates the mean concentration species, i.e., their logarithm, for each grid cell as follows:

$$\ln(\overline{C}_{ij}) = \frac{1}{\sum_{k=1}^{N} \tau_{ijk}} \sum_{k=1}^{N} \ln(c_k)\, \tau_{ijk}$$

where i and j are the indices of grid, k the index of trajectory, N the total number of trajectories used in analysis, c_k the pollutant concentration measured upon arrival of trajectory k, and τ_{ijk} the residence time of trajectory k in grid cell (i, j). With this CWT method, air packets that stay longer in a cell are weighted higher, which is not the case for PSCF. Additionally, the PSCF method requires a weighting function for multi-site analysis, which remains a challenge. Furthermore, as previously mentioned, PSCF relies on an arbitrary threshold, causing the model to emphasize high-source contributions. This can result in an imbalanced representation of moderate and relatively high source contributions. For these reasons, we have chosen to use CWT for the purpose of this study. A high value of $\overline{C}_{ij}$ means that air parcels passing over cell (i, j) would, on average, cause high concentrations at the receptor site (Carslaw, 2019; Wilks, 2019).

2.3 Air quality modelling

An atmospheric chemistry transport model (CAMx) (Yarwood et al., 2024) was deployed to simulate the distribution and transport of air pollutants for the year 2017. Also, as shown in Figure S8, the spatial variabilities and pollution hotspots (including Po Valley) for CAMx modelling results in 2013 and 2017 are relatively consistent. We chose that particular year because it had the largest overlap of the ACSM/AMS data (see Figure 1), making it more suitable for comparison with the TSM analysis. In addition, one year of modelling results should cover most of the relevant scenarios of meteorological conditions. The model domain covers nearly all Europe (Figure 2),

with a horizontal resolution of 0.25 x 0.125 degrees (lon x lat) and 14 vertical layers from the near surface to 7 km ASL. The high-resolution (0.1 x 0.1 degree) European emission inventory, Copernicus Atmosphere Monitoring Service-Regional Inventory-Version 4, developed by the Netherlands TNO (Kuenen et al., 2022a), is deployed in the simulation. The gas phase chemistry is simulated using the Carbon Bond 6 Revision 2 mechanism (Hildebrandt Ruiz & Yarwood, 2013). The ISORROPIA model (Nenes et al., 1998) is used to simulate the thermodynamic and gas-particle partitioning of inorganic aerosols. Future studies should consider using a more advanced mechanism (e.g., ISORROPIA II (Fountoukis & Nenes, 2007)) to improve the model performance on SIA. Simulation of secondary organic aerosols is carried out using a 1.5-dimensional volatility basis set module (Koo et al., 2014). The CAMx model is driven by the hourly meteorology from the regional Weather Research and Forecasting model (WRF, version 3.7), which is driven by and nudged to a 6-hourly reanalysis of global meteorology from the European Centre for Medium-range Weather Forecasts. The chemistry initial and boundary conditions for CAMx are provided by the MOZART4 global model (Horowitz et al., 2003). The CAMx model and the used configuration have been validated in many previous studies to well reproduce the air pollution over Europe (Daellenbach et al., 2020, 2023; Jiang et al., 2019a; Jiang et al., 2019b). More details of model configuration and validation are given in our previous research (Daellenbach et al., 2020; Jiang et al., 2019a; Jiang et al., 2019b).

3 Results and Discussion

The frequencies of the trajectories, without the concentrations, are presented in Figure 2. Figure 3 shows the yearly averaged results for the different species (BBOA, OOA, total organics, NH_4, NO_3, SO_4). For each species, the plot on the left-hand side displays the result of the TSM analysis, i.e., the specific source areas. On the right-hand side, respectively, we have plotted the specific local concentrations as simulated by CAMx (Jiang et al., 2019b). Additionally, emission inventories of a few selected species can be found in Figure S1. We have decided to focus here on the comparison with the simulated concentrations in order to obtain a comprehensive picture of both the source regions and those most affected by air pollution. Note that the scales for the TSM and CAMx results are different in Figure 3, in order to visualise better some of the patterns. Figure S2 shows the side-by-side comparisons with the same scaling. Figure 4 contains the seasonal plots for June, July, August (JJA) and December, January, February (DJF) of BBOA, NO_3, and SO_4, all of which we expected strong seasonality.

Firstly, looking at the frequency plot (Figure 2), we notice that the highest percentage of trajectories are very close to the actual measurement stations, which is what we would expect. A significant percentage of trajectories are over continental Europe, and there are also some over the Atlantic. Overall, Figure 2 indicates a decent coverage of the air masses over the European domain of interest.

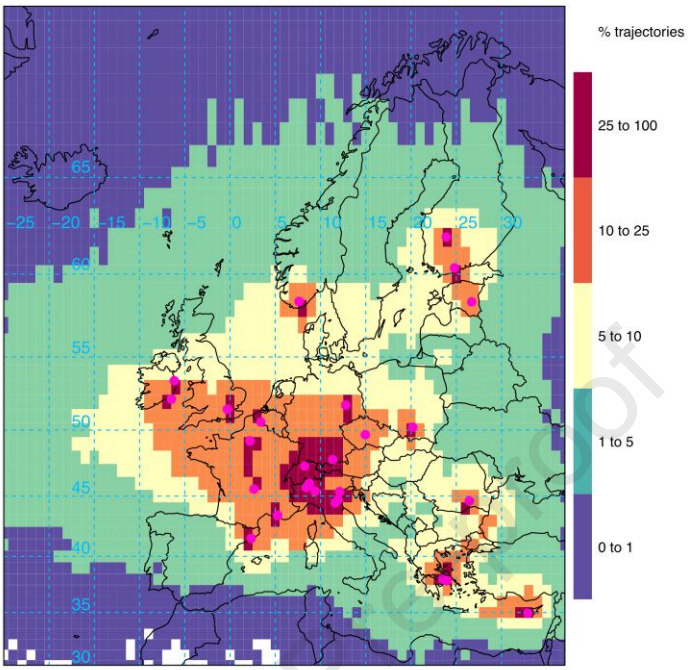

277

278 **Fig. 2.** Frequency plot of the trajectories without the concentrations. The colours indicate the
279 percentages of the total amount of trajectories passing through each grid cell. The pink dots
280 indicate the locations of the measurement sites.

281 It is important to note that in our analysis, all of the available ACSM/AMS data were used with
282 the CWT method in a single run, not accounting for different campaign durations and times. As
283 can be seen in Figure 1, some sites have much shorter campaigns and fewer data points in overall
284 comparison. Even though the CWT method weighs according to concentrations, not the number
285 of measurement points, this could still potentially lead to an underestimation of shorter campaigns.
286 To study this limitation, we have conducted different analyses, which are included in the
287 supplementary. Firstly, Figure S3 shows the year-round TSM analysis for only the stations in the
288 Po Valley, which had shorter campaigns compared to other regions. Figure S4 shows the results
289 of the TSM analysis for only the month of January with the most overlapping measurements in the
290 Po Valley, averaged over all years. Figure S5 again shows only the January average, excluding the

stations in Krakow and Bucharest. Comparing Figure S4 with the original DJF plots for BBOA, NO_3, and SO_4, we see that the overall picture does not change significantly. Even excluding Krakow and Bucharest from the analysis (Figure S5) only changes the scaling, not the source regions highlighted. Comparing measurements from different times and of different durations definitely poses a challenge, and we acknowledge this limitation, which is generally difficult to quantify, in our analysis. But seeing that our results are sufficiently robust under different circumstances gives us confidence in our approach and its ability to identify aerosol source regions, while also allowing for a straightforward integration of datasets in the future. Nonetheless, we highlight the need for long-term measurement datasets and a wide-spread network of stations.

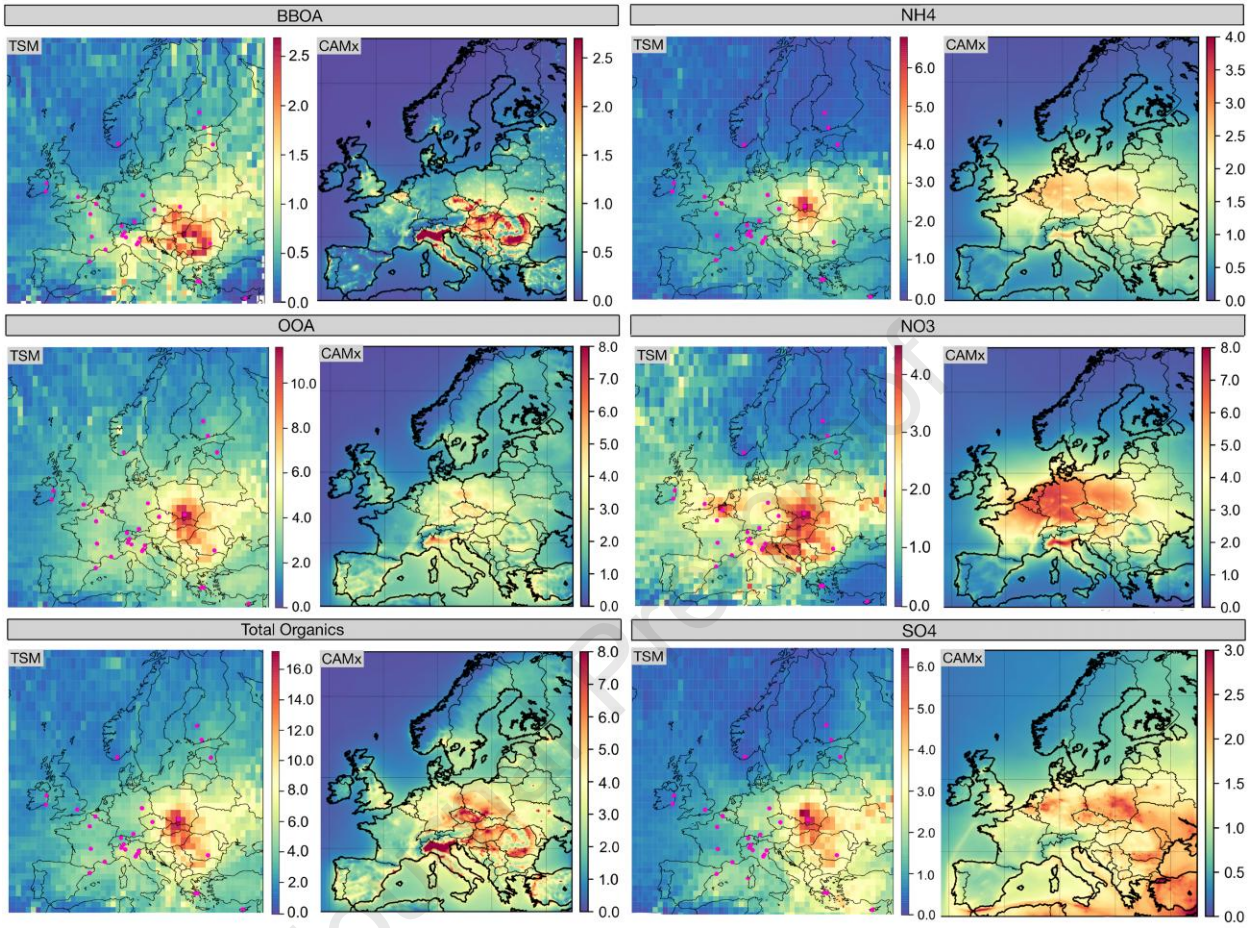

Fig. 3. Comparison of year-round TSM and CAMx results for BBOA, OOA, total OA, NH_4, NO_3, and SO_4. Color scale is in $\mu g \cdot m^{-3}$.

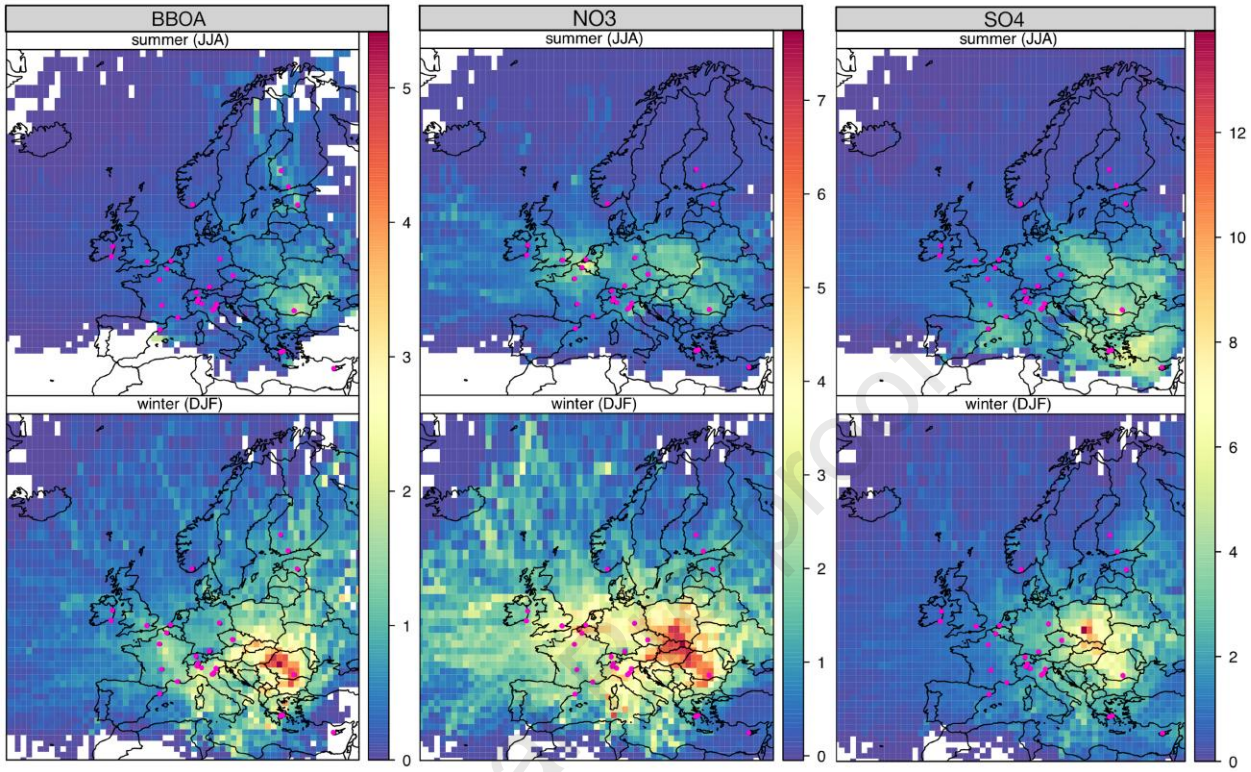

Fig. 4. Seasonal plots showing TSM results for BBOA, NO_3, and SO_4, with summer results on top and winter results on the bottom. Color scale is in $\mu g \cdot m^{-3}$.

3.1 BBOA

The results of the TSM analysis show that most of the contributions are from continental Europe. This is what we would expect since BBOA is only emitted over land. Most notably, the highest contributions come from Eastern Europe, stretching from southern Poland to northern Greece. There is hardly anything from Western Europe.

In agreement with the TSM predictions, high BBOA concentrations were predicted in Eastern Europe by CAMx, in particular in Hungary, Romania, and the Balkans. This would suggest that most of the BBOA emitted in those regions stays local as it's highly reactive in the atmosphere (Hennigan et al., 2010) and oxidises quickly. We can also observe concentration hotspots around

major cities. The most significant difference between CAMx and TSM predictions can be observed in the Po Valley, where CAMx estimates a high BBOA concentration while not being elevated as a source region by the TSM analysis. When including the PMF results for Po Valley in the analysis we find a marginal increase in concentrations in those regions (Figure S3), compared to the analysis without those 5 sites. However, this region is still not at the same level of concentration as Eastern Europe. In the Po Valley, CAMx might underestimate oxidation processes leading to the formation of OOA from BBOA, an important source of OOA as described in Paglione et al. (2020). Also, CAMx utilizes meteorological data from the European Centre for Medium-Range Weather Forecasts (ECMWF), while the TSM implements NOAA's GDAS dataset, potentially leading to a different transport of air masses into and out of the Po Valley. The strongest hypothesis for the overestimation of BBOA in the Po Valley in CAMx is, however, that the model failed to catch fog scavenging processes (Gilardoni et al., 2014), which leads to a general overestimation of total organics (Jiang et al., 2019a). As we include multiple different sites in the TSM analysis, we conclude that, relatively, the Po Valley is a less important source region of BBOA than Eastern Europe.

Figure 4 shows high BBOA concentrations in winter, indicating the importance of domestic heating sources. We can also see a high contribution from Finland in the summer.

3.2 OOA

Our analysis indicates that OOA mainly originates from continental Europe, with the highest concentrations observed in Eastern Europe (from southern Poland to Romania). Although Chen et al. (2022) reported exceptionally high concentrations measured by the Krakow station, excluding

this station from our analysis did not significantly alter the results, as illustrated in Figure S6. Therefore, we can confidently conclude that these regions indeed serve as hotspots for OOA.

CAMx also indicates high concentrations in Eastern Europe, particularly in the Czech Republic, indicating a more local effect of OOA sources. This can also be seen in Hungary and southern Romania, which are both elevated by the CAMx and TSM approaches. While the CAMx predicts high concentrations in the Po Valley, the TSM observed comparatively low contributions from this region. The overestimation of primary OA sources in general by CAMx, and the exclusion of fog scavenging processes (Gilardoni et al., 2014; Jiang, et al., 2019b), may lead to overall higher production of OOA in the Po Valley than what was simulated by CAMx. Once again, this could suggest that the Po Valley does not contribute much to the overall air pollution burden in Europe. Despite surrounding stations, the TSM did not predict significant contributions from Turkey, even though CAMx predicts high concentrations. This could possibly be due to limited trajectories passing through this region, as depicted in Figure 2.

3.3 Total organics

A distinct east-west contrast in OA concentrations is evident in both CAMx and TSM approaches, which indicates that OA is not transported over the entire continent. OA contributions primarily originate from continental Europe, notably southern Poland, extending to Serbia and northern Bulgaria. CAMx also predicts high OA concentrations in that region, in addition to the Benelux, parts of Germany, the Po Valley, and Turkey. It also depicts localised high OA concentrations around major cities, beyond the resolution of the TSM analysis. The TSM highlights concentrations exceeding 16 $\mu g \cdot m^{-3}$ over Poland, compared to simulations reaching only up to 4

358 μg·m^{-3}. This disparity could be attributed to exceptionally high concentrations around Krakow
359 (Tobler et al., 2021), which might disproportionately affect the TSM analysis. However,
360 performing the TSM analysis without the Krakow station (Figure S6) still highlights Eastern
361 Europe as the main source region. This could indicate inconsistencies in long-range transport of
362 air masses between CAMx and TSM due to the different meteorological datasets used. Or, it might
363 suggest a tendency for CAMx to underestimate actual OA levels in southern Poland. Indeed, the
364 emission inventory of CAMx does not include coal combustion, which is a significant emission
365 source particularly in Eastern Europe. Yet, multi-site observations from this region would be
366 needed to confirm this tendency. In addition, the emission inventory we used as model inputs
367 (TNO-CAMS) was 102% lower than EDGAR emissions in non-EU countries (Kuenen et al.,
368 2022b), which may also lead to underestimation of OA, for example in Serbia.

369 ### *3.4 NH_4*

370 Our TSM analysis shows the highest NH_4 contributions from the region in and around Krakow.
371 Overall, Eastern Europe is rather elevated, as are some regions in Western Europe, such as the
372 Benelux and Germany. The highest CAMx concentrations are over Belgium, Germany, Czechia,
373 the Po Valley, and Poland, with some slightly elevated concentrations over the southeast of the
374 UK, Northern France, Slovakia, Balkan regions, Ukraine, the south of Romania, and Turkey.
375 Overall, both approaches show a consistent spatial distribution except for the Po Valley, indicating
376 that the emission inventory for CAMx is in agreement with the measurements. For the Po Valley,
377 the differences in meteorology including missing fog scavenging (Gilardoni et al., 2014; Jiang, et
378 al., 2019) as mentioned above, most likely lead to the discrepancies between CAMx and the TSM

model. The latter also generally showed pronounced contributions of PM components in southern Poland, which leads to higher NH_4 concentrations than the CAMx model (Figure S2). From Figure 3, we see that SO_4 shows higher concentrations for the TSM model results than for CAMx, due to lack of coal combustion source in CAMx. NH_4 and SO_4 were found to be correlated, because they both depend on neutralization processes (Shon et al., 2020). NH_4 concentrations in CAMx might also be directly affected by the underestimation of coal combustion emissions (Z. Chen et al., 2022). NO_3

In the TSM analysis, we observe significant contributions from northern France, the Benelux region, and Eastern Europe, which align with the expected patterns given the influence of high NO_x and NH_3 emissions from urban areas, particularly those with heavy traffic. Surprisingly, we also detected relatively elevated contributions from the Atlantic, which prompted further investigation. Upon conducting our analysis without data from select stations in the UK, Ireland, Paris, and Lille, we found that this oceanic influence vanished, as illustrated in Figure S7. This suggests that these unexpected findings are likely artefacts of the TSM process. Additionally, trajectory analysis (see Figure 2) reveals a notable proportion of trajectories passing over the Atlantic, corroborating our assessment. As expected, NO_3 exhibits a significant seasonal trend, with higher concentrations in winter due to enhanced partitioning at lower temperatures (Figure 4) (Bressi et al., 2021; Poulain et al., 2011)

We observe that CAMx estimated concentrations of NO_3 are considerably higher than the TSM model across the UK, northern France,Germany, and Czechia, potentially caused by scarcities of measurements in those regions, leading to an underestimation in the TSM analysis. There are some agreements between CAMx and TSM modelin the Benelux region, Eastern Europe and Southern

Europe (Figure S2). The discrepancy between CAMx and TSM model in the Po Valley, with significantly higher concentrations from the CAMx simulations, could again be caused by the different meteorological datasets includingthe lack of fog scavenging.

3.5 SO_4

In winter, the TSM model predicts the highest concentrations over Eastern Europe, particularly in Poland, likely due to industrial emissions and residential coal burning for heating (Figures 3 and 4). Significant contributions are also observed from the Mediterranean region, attributed to high ship emissions and enhanced photochemistry during the summer in this region (Figures 3 and 4). There is a match of hotspots between the TSM and CAMx simulations over Poland, the Balkans, the Mediterranean, and Turkey. However, the TSM model showed much higher concentrations than CAMx in Eastern Europe due to the potential underestimation of the CAMx model from industrial and coal combustion sources. In addition, the CAMx model might slightly underestimate ship exhaust near the Aegean Sea and southwest of Turkey's coastline, resulting in relatively higher concentrations in these regions for the TSM model. Nevertheless, SO_4 could still be underestimated in the Balkans, where coal power plants are quite a common source due to both the scarcity of measurements in this region and limitations of the emission inventories. Indeed, the model underestimation of SO_4 is a known issue for many air quality models (Im et al., 2015). A primary explanation is the lack of accurate heterogeneous formation mechanisms in the model (Miao et al., 2020). Meanwhile, uncertainties in emissions, meteorological fields and deposition processes can all contribute to model bias. From Figure S1 we see that Eastern Europe and the Balkans are exactly the regions with intensive SO_2 emissions. Those regions reportedly have a

larger uncertainty in SO_2 emissions than for example western European countries (Vestreng et al., 2007). In addition, other species like NH_3 could also influence the model performance in SO_4 by mediating the chemical reactions. The emission inventory we used as model inputs (TNO-CAMS) was 102% lower than EDGAR emissions in non-EU countries (Kuenen et al., 2022b), which may also lead to underestimation of SO_4. The TSM results for SO_4 in the UK show less pronounced contributions compared to the high concentrations predicted by CAMx, indicating a potential overestimation of SO_2 emissions in these regions.

4 Conclusion

In this study, we investigated various PM components, both organic (BBOA, OOA, and total OA) and inorganic (NH_4, NO_3, SO_4), and their long-range transport in Europe. Our aim was to identify their geographical origins by combining source apportionment results and measurements from 27 air quality observational sites with TSMs. Using numerous trajectories and receptors reduced uncertainties, providing a comprehensive analysis of source origins. We then compared these results to estimations of concentrations by the CAMx air quality model in Europe. However, we acknowledge the caveat of this analysis to combine several receptors with different time periods, and the fact that back trajectory analysis does not reproduce all atmospheric physicochemical processes.

Starting with the organic components, most contributions come from continental Europe. BBOA hotspots are around southern Poland to northern Greece. The main source regions as predicted by our analysis mostly align well with regions of high concentrations as simulated by CAMx, except

for the Po Valley. Seasonally, concentrations are low in summer and high in winter, likely due to heating. For OOA, the highest contributions are also from Eastern Europe, in particular southern Poland to Romania. The CAMx also highlights this region, but predicts overall lower absolute concentrations, which could indicate transport processes. Excluding the Poland station did not change results, suggesting this region is a major contributor, possibly also underestimated in the CAMx model. The TSM analysis also shows discrepancies with the CAMx results in the Po Valley, potentially indicating an overestimation in the CAMx model, or transport processes. For total organics, the highest contributions are from southern Poland to Bulgaria, with a clear east-west contrast well captured by our TSM analysis. Overall, Eastern Europe seems to be the most important contributor.

For inorganic components, NH4 shows high contributions from Poland, and the TSM results generally match predictions of regions with high concentrations from CAMx except for Po Valley. The NO_3 contribution is highest from northern France, Benelux, and Eastern Europe due to NO_x emissions from traffic and agricultural emissions in Benelux. The CAMx results show higher concentrations than the TSM analysis in northern Europe, and Po Valley with good consistences in Eastern Europe in general. TSM analysis showed lower NO_3 concentrations in summer, likely due to higher temperatures, photochemistry keeping NO_3 in the gas phase, and higher vertical dilution. SO_4 concentrations are high in Poland, likely from industrial and heating emissions, and over the Mediterranean, due to photochemistry and ship exhausts. This matches CAMx model highlights, though we do not find elevated concentrations over Benelux and Germany. Seasonally, SO_4 is higher in winter over Poland and in summer over the Mediterranean, supporting heating-related emissions and the photochemical transformation of SO_2 to SO_4, respectively.

In conclusion, we have developed a novel approach to take advantage of available large datasets to have a comprehensive picture of the geographical origins of different PM components, such as BBOA, OOA, total OA, NH_4, NO_3, and SO_4 across Europe. It demonstrated great consistency with the concentrations simulated by the CAMx model. With the help of more data available in the future, the results of this analysis could be used to validate and improve the emission inventories of air quality chemical transport models. By understanding the intricate interplay between local emissions and long-range transport, stakeholders can implement informed strategies to improve air quality on a larger scale, protect human health, and safeguard ecosystems in both source and receptor regions.

Data availability

The code to execute the TSM analysis can be found in the supporting material. Raw data of the TSM data is publicly available through Zenodo: https://zenodo.org/records/6672710. The raw data of CAMx results are available through a request to the corresponding authors.

Acknowledgements

The authors gratefully acknowledge the Swiss data science center (grant C08-20, Aurora), the Swiss federal office of environment (FOEN) and the Joint Research Program of the Swiss National Science Foundation (SNSF grant no. 189883) for their financial support. We want to thank CNRS-INSU for supporting measurements performed at the SI-COPDD, and those within the long-term monitoring aerosol program SNO-CLAP, both of which are components of the ACTRIS French

Research Infrastructure, and whose data is hosted at the AERIS data center (https://www.aeris-data.fr/). We further acknowledge EPA Ireland and the Department of Environment, Climate and Communications, Horizon Europe (grant no. 101081430 - PARIS), as well as the National Key Research and Development Program of China (2023YFC3710400), and the National Natural Science Foundation of China (42207122). Additionally, this work is supported by the Core Program within the Romanian National Research Development and Innovation Plan 2022-2027, carried out with the support of MCID, project no. PN 23 05). Hasna Chebaicheb's PhD grant is supported by the LCSQA funded by the French Ministry of Environment. IMTNord Europe acknowledges financial support from the Labex CaPPA project, which is funded by the French National Research Agency (ANR) through the PIA (Programme d'Investissement d'Avenir) under contract ANR-11-LABX-0005-01, and the CLIMIBIO and ECRIN projects, both financed by the Regional Council "Hauts-de-France" and the European Regional Development Fund (ERDF). All co-authors participated in or supported by the COST COLOSSAL Action CA16109. The ATOLL site is one of the French ACTRIS National Facilities and contributes to the CARA program of the LCSQA funded by the French Ministry of Environment. Mikael Ehn, Liine Heikkinen, Minna Aurela, and Hilkka Timonen are funded by Research Council of Finland (grants 317380, 345982, 337549, 3570902 and 357905).

Lastly, we want to mention the invaluable work by the following people: Andres Alastuey (andres.alastuey@idaea.csic.es) from CSIC, Gregory Gille (gregory.gille@atmosud.org) from Atmosud, Erik Teinemaa (erik.teinemaa@klab.ee) from Estonian Environmental Research Centre (EERC), Anja Tremper (anja.tremper@imperial.ac.uk) and Max Priestman

504 (m.priestman@imperial.ac.uk) from the MRC Centre for Environment and Health at Imperial
505 College London.

506

References

Bressi, M., Cavalli, F., Putaud, J. P., Fröhlich, R., Petit, J. E., Aas, W., Äijälä, M., Alastuey, A., Allan, J. D., Aurela, M., Berico, M., Bougiatioti, A., Bukowiecki, N., Canonaco, F., Crenn, V., Dusanter, S., Ehn, M., Elsasser, M., Flentje, H., … Prevot, A. S. H. (2021). A European aerosol phenomenology - 7: High-time resolution chemical characteristics of submicron particulate matter across Europe. *Atmospheric Environment: X*, *10*, 100108. https://doi.org/10.1016/J.AEAOA.2021.100108

Calvin, K., Dasgupta, D., Krinner, G., Mukherji, A., Thorne, P. W., Trisos, C., Romero, J., Aldunce, P., Barrett, K., Blanco, G., Cheung, W. W. L., Connors, S., Denton, F., Diongue-Niang, A., Dodman, D., Garschagen, M., Geden, O., Hayward, B., Jones, C., … Ha, M. (2023). *IPCC, 2023: Climate Change 2023: Synthesis Report. Contribution of Working Groups I, II and III to the Sixth Assessment Report of the Intergovernmental Panel on Climate Change [Core Writing Team, H. Lee and J. Romero (eds.)]. IPCC, Geneva, Switzerland.* https://doi.org/10.59327/IPCC/AR6-9789291691647

Carslaw, D. (2019). *The openair manual open-source tools for analysing air pollutiondata*. https://github.com/davidcarslaw/openair.

Chen, G., Canonaco, F., Tobler, A., Aas, W., Alastuey, A., Allan, J., Atabakhsh, S., Aurela, M., Baltensperger, U., Bougiatioti, A., De Brito, J. F., Ceburnis, D., Chazeau, B., Chebaicheb, H., Daellenbach, K. R., Ehn, M., El Haddad, I., Eleftheriadis, K., Favez, O., … Prévôt, A. S. H. (2022). European aerosol phenomenology − 8: Harmonised source apportionment of

organic aerosol using 22 Year-long ACSM/AMS datasets. *Environment International*, *166*, 107325. https://doi.org/10.1016/j.envint.2022.107325

Chen, Y., Beig, G., Archer-Nicholls, S., Drysdale, W., Acton, W. J. F., Lowe, D., Nelson, B., Lee, J., Ran, L., Wang, Y., Wu, Z., Sahu, S. K., Sokhi, R. S., Singh, V., Gadi, R., Nicholas Hewitt, C., Nemitz, E., Archibald, A., McFiggans, G., & Wild, O. (2021). Avoiding high ozone pollution in Delhi, India. *Faraday Discussions*, *226*, 502–514. https://doi.org/10.1039/D0FD00079E

Chen, Z.-L., Song, W., Hu, C.-C., Liu, X.-J., Chen, G.-Y., Walters, W. W., Michalski, G., Liu, C.-Q., Fowler, D., & Liu, X.-Y. (2022). Significant contributions of combustion-related sources to ammonia emissions. *Nature Communications*, *13*(1), 7710. https://doi.org/10.1038/s41467-022-35381-4

COST Action CA16109 COLOSSAL Chemical On-Line cOmposition and Source Apportionment of fine aerosoL, W. G. 1. (2021, May). *Quadrupole Aerosol Chemical Speciation Monitor (Q-ACSM) - Standard Operating Procedure*. https://www.actris-ecac.eu/

COST Action CA16109 COLOSSAL Chemical On-Line cOmposition and Source Apportionment of fine aerosoL, W. G. 1. (2022, March). *Time of Flight Aerosol Chemical Speciation Monitors (TOF-ACSM) - Standard Operating Procedure*. https://www.actris-ecac.eu/

Crenn, V., Sciare, J., Croteau, P. L., Verlhac, S., Fröhlich, R., Belis, C. A., Aas, W., Äijälä, M., Alastuey, A., Artiñano, B., Baisnée, D., Bonnaire, N., Bressi, M., Canagaratna, M., Canonaco, F., Carbone, C., Cavalli, F., Coz, E., Cubison, M. J., … Favez, O. (2015). ACTRIS ACSM intercomparison – Part 1: Reproducibility of concentration and fragment results from 13 individual Quadrupole Aerosol Chemical Speciation Monitors (Q-ACSM) and

consistency with co-located instruments. *Atmospheric Measurement Techniques*, *8*(12), 5063–5087. https://doi.org/10.5194/amt-8-5063-2015

Crippa, M., Canonaco, F., Lanz, V. A., Äijälä, M., Allan, J. D., Carbone, S., Capes, G., Ceburnis, D., Dall'Osto, M., Day, D. A., DeCarlo, P. F., Ehn, M., Eriksson, A., Freney, E., Hildebrandt Ruiz, L., Hillamo, R., Jimenez, J. L., Junninen, H., Kiendler-Scharr, A., … Prévôt, A. S. H. H. (2014). Organic aerosol components derived from 25 AMS data sets across Europe using a consistent ME-2 based source apportionment approach. *Atmospheric Chemistry and Physics*, *14*(12), 6159–6176. https://doi.org/10.5194/acp-14-6159-2014

Daellenbach, K. R., Manousakas, M., Jiang, J., Cui, T., Chen, Y., El Haddad, I., Fermo, P., Colombi, C., & Prévôt, A. S. H. (2023). Organic aerosol sources in the Milan metropolitan area – Receptor modelling based on field observations and air quality modelling. *Atmospheric Environment*, *307*, 119799. https://doi.org/10.1016/j.atmosenv.2023.119799

Daellenbach, K. R., Uzu, G., Jiang, J., Cassagnes, L.-E., Leni, Z., Vlachou, A., Stefenelli, G., Canonaco, F., Weber, S., Segers, A., Kuenen, J. J. P., Schaap, M., Favez, O., Albinet, A., Aksoyoglu, S., Dommen, J., Baltensperger, U., Geiser, M., El Haddad, I., … Prévôt, A. S. H. (2020). Sources of particulate-matter air pollution and its oxidative potential in Europe. *Nature*, *587*(7834), 414–419. https://doi.org/10.1038/s41586-020-2902-8

Draxler, R. R. (1999). *HYSPLIT4 User's Guide*. https://www.arl.noaa.gov/documents/reports/hysplit_user_guide.pdf

Drewnick, F., Hings, S. S., DeCarlo, P., Jayne, J. T., Gonin, M., Fuhrer, K., Weimer, S., Jimenez, J. L., Demerjian, K. L., Borrmann, S., & Worsnop, D. R. (2005). A New Time-of-Flight Aerosol Mass Spectrometer (TOF-AMS)—Instrument Description and First Field

571 Deployment. *Aerosol Science and Technology*, *39*(7), 637–658.
572 https://doi.org/10.1080/02786820500182040
573 Escudero, M., Stein, A. F., Draxler, R. R., Querol, X., Alastuey, A., Castillo, S., & Avila, A.
574 (2011). Source apportionment for African dust outbreaks over the Western Mediterranean
575 using the HYSPLIT model. *Atmospheric Research*, *99*(3–4), 518–527.
576 https://doi.org/10.1016/j.atmosres.2010.12.002
577 Fountoukis, C., & Nenes, A. (2007). ISORROPIA II: a computationally efficient thermodynamic
578 equilibrium model for K^+–Ca^{2+}–Mg^{2+}–NH_4^+–Na^+–SO_4^{2-}–NO_3^-–Cl^-–H_2O
579 aerosols. *Atmospheric Chemistry and Physics*, *7*(17), 4639–4659.
580 https://doi.org/10.5194/acp-7-4639-2007
581 Freney, E., Zhang, Y., Croteau, P., Amodeo, T., Williams, L., Truong, F., Petit, J.-E., Sciare, J.,
582 Sarda-Esteve, R., Bonnaire, N., Arumae, T., Aurela, M., Bougiatioti, A., Mihalopoulos, N.,
583 Coz, E., Artinano, B., Crenn, V., Elste, T., Heikkinen, L., … Favez, O. (2019). The second
584 ACTRIS inter-comparison (2016) for Aerosol Chemical Speciation Monitors (ACSM):
585 Calibration protocols and instrument performance evaluations. *Aerosol Science and*
586 *Technology*, *53*(7), 830–842. https://doi.org/10.1080/02786826.2019.1608901
587 Fröhlich, R., Crenn, V., Setyan, A., Belis, C. A., Canonaco, F., Favez, O., Riffault, V., Slowik, J.
588 G., Aas, W., Aijälä, M., Alastuey, A., Artiñano, B., Bonnaire, N., Bozzetti, C., Bressi, M.,
589 Carbone, C., Coz, E., Croteau, P. L., Cubison, M. J., … Prévôt, A. S. H. (2015). ACTRIS
590 ACSM intercomparison – Part 2: Intercomparison of ME-2 organic source apportionment
591 results from 15 individual, co-located aerosol mass spectrometers. *Atmospheric Measurement*
592 *Techniques*, *8*(6), 2555–2576. https://doi.org/10.5194/amt-8-2555-2015

Fröhlich, R., Cubison, M. J., Slowik, J. G., Bukowiecki, N., Prévôt, A. S. H., Baltensperger, U., Schneider, J., Kimmel, J. R., Gonin, M., Rohner, U., Worsnop, D. R., & Jayne, J. T. (2013). The ToF-ACSM: a portable aerosol chemical speciation monitor with TOFMS detection. *Atmospheric Measurement Techniques*, *6*(11), 3225–3241. https://doi.org/10.5194/amt-6-3225-2013

GDAS. (n.d.). *Global Data Assimilation System (GDAS) | National Centers for Environmental Information (NCEI)*. Retrieved January 11, 2025, from https://www.ncei.noaa.gov/products/weather-climate-models/global-data-assimilation

Gilardoni, S., Massoli, P., Giulianelli, L., Rinaldi, M., Paglione, M., Pollini, F., Lanconelli, C., Poluzzi, V., Carbone, S., Hillamo, R., Russell, L. M., Facchini, M. C., & Fuzzi, S. (2014). Fog scavenging of organic and inorganic aerosol in the Po Valley. *Atmospheric Chemistry and Physics*, *14*(13), 6967–6981. https://doi.org/10.5194/acp-14-6967-2014

Harrison, R. M., & Yin, J. (2000). Particulate matter in the atmosphere: which particle properties are important for its effects on health? *Science of The Total Environment*, *249*(1–3), 85–101. https://doi.org/10.1016/S0048-9697(99)00513-6

Hennigan, C. J., Sullivan, A. P., Collett, J. L., & Robinson, A. L. (2010). Levoglucosan stability in biomass burning particles exposed to hydroxyl radicals. *Geophysical Research Letters*, *37*(9), 2–5. https://doi.org/10.1029/2010GL043088

Hildebrandt Ruiz, L., & Yarwood, G. (2013). Interactions between organic aerosol and NOy: Influence on oxidant production. *Final Report Prepared for the Texas Air Quality Research Program (Project 12-012) by the University of Texas at Austin and ENVIRON International Corporation*.

615 Horowitz, L. W., Walters, S., Mauzerall, D. L., Emmons, L. K., Rasch, P. J., Granier, C., Tie, X.,
616 Lamarque, J., Schultz, M. G., Tyndall, G. S., Orlando, J. J., & Brasseur, G. P. (2003). A global
617 simulation of tropospheric ozone and related tracers: Description and evaluation of
618 MOZART, version 2. *Journal of Geophysical Research: Atmospheres*, *108*(D24).
619 https://doi.org/10.1029/2002JD002853
620 Hsu, Y.-K., Holsen, T. M., & Hopke, P. K. (2003). Comparison of hybrid receptor models to locate
621 PCB sources in Chicago. *Atmospheric Environment*, *37*(4), 545–562.
622 https://doi.org/10.1016/S1352-2310(02)00886-5
623 Im, U., Bianconi, R., Solazzo, E., Kioutsioukis, I., Badia, A., Balzarini, A., Baró, R., Bellasio, R.,
624 Brunner, D., Chemel, C., Curci, G., Denier van der Gon, H., Flemming, J., Forkel, R.,
625 Giordano, L., Jiménez-Guerrero, P., Hirtl, M., Hodzic, A., Honzak, L., … Galmarini, S.
626 (2015). Evaluation of operational online-coupled regional air quality models over Europe and
627 North America in the context of AQMEII phase 2. Part II: Particulate matter. *Atmospheric*
628 *Environment*, *115*, 421–441. https://doi.org/10.1016/j.atmosenv.2014.08.072
629 Jiang, J., Aksoyoglu, S., Ciarelli, G., Oikonomakis, E., El-Haddad, I., Canonaco, F., O'Dowd, C.,
630 Ovadnevaite, J., Minguillón, M. C., Baltensperger, U., & Prévôt, A. S. H. (2019). Effects of
631 two different biogenic emission models on modelled ozone and aerosol concentrations in
632 Europe. *Atmospheric Chemistry and Physics*, *19*(6), 3747–3768. https://doi.org/10.5194/acp-
633 19-3747-2019
634 Jiang, J., Aksoyoglu, S., El-Haddad, I., Ciarelli, G., Denier van der Gon, H. A. C., Canonaco, F.,
635 Gilardoni, S., Paglione, M., Minguillón, M. C., Favez, O., Zhang, Y., Marchand, N., Hao, L.,
636 Virtanen, A., Florou, K., O'Dowd, C., Ovadnevaite, J., Baltensperger, U., & Prévôt, A. S. H.

(2019). Sources of organic aerosols in Europe: a modeling study using CAMx with modified volatility basis set scheme. *Atmospheric Chemistry and Physics*, *19*(24), 15247–15270. https://doi.org/10.5194/acp-19-15247-2019

Jimenez, J. L., Canagaratna, M. R., Donahue, N. M., Prevot, A. S. H. H., Zhang, Q., Kroll, J. H., DeCarlo, P. F., Allan, J. D., Coe, H., Ng, N. L., Aiken, A. C., Docherty, K. S., Ulbrich, I. M., Grieshop, A. P., Robinson, A. L., Duplissy, J., Smith, J. D., Wilson, K. R., Lanz, V. A., … Worsnop, D. R. (2009). Evolution of Organic Aerosols in the Atmosphere. *Science*, *326*(5959), 1525–1529. https://doi.org/10.1126/science.1180353

Koo, B., Knipping, E., & Yarwood, G. (2014). 1.5-Dimensional volatility basis set approach for modeling organic aerosol in CAMx and CMAQ. *Atmospheric Environment*, *95*, 158–164. https://doi.org/10.1016/j.atmosenv.2014.06.031

Kuenen, J., Dellaert, S., Visschedijk, A., Jalkanen, J.-P., Super, I., & Denier van der Gon, H. (2022a). CAMS-REG-v4: a state-of-the-art high-resolution European emission inventory for air quality modelling. *Earth System Science Data*, *14*(2), 491–515. https://doi.org/10.5194/essd-14-491-2022

Kuenen, J., Dellaert, S., Visschedijk, A., Jalkanen, J.-P., Super, I., & Denier van der Gon, H. (2022b). CAMS-REG-v4: a state-of-the-art high-resolution European emission inventory for air quality modelling. *Earth System Science Data*, *14*(2), 491–515. https://doi.org/10.5194/essd-14-491-2022

Lee, S., & Ashbaugh, L. (2007). Comparison of multi-receptor and single-receptor trajectory source apportionment (TSA) methods using artificial sources. *Atmospheric Environment*, *41*(6), 1119–1127. https://doi.org/10.1016/j.atmosenv.2006.10.019

659 Liu, X., Lara, R., Dufresne, M., Wu, L., Zhang, X., Wang, T., Monge, M., Reche, C., Di Leo, A.,
660 Lanzani, G., Colombi, C., Font, A., Sheehan, A., Green, D. C., Makkonen, U., Sauvage, S.,
661 Salameh, T., Petit, J.-E., Chatain, M., … Querol, X. (2024). Variability of ambient air
662 ammonia in urban Europe (Finland, France, Italy, Spain, and the UK). *Environment*
663 *International*, *185*, 108519. https://doi.org/10.1016/j.envint.2024.108519
664 Lupu, A., & Maenhaut, W. (2002). Application and comparison of two statistical trajectory
665 techniques for identification of source regions of atmospheric aerosol species. *Atmospheric*
666 *Environment*, *36*(36–37), 5607–5618. https://doi.org/10.1016/S1352-2310(02)00697-0
667 Mărmureanu, L., Marin, C. A., Vasilescu, J., Petit, J.-E., Amodeo, T., Truong, F., Antonescu, B.,
668 Minguillon, M. C., Green, D. C., Zainab, B., Ovadnevaite, J., Elste, T., Coz, E., Allan, J.,
669 Croteau, P. L., Jayne, J., Canagaratna, M. R., Williams, L., Gros, V., … Freney, E. (2025).
670 Evaluation of aerosol chemical speciation monitor response to different mixtures of organic
671 and inorganic aerosols. *Aerosol Science and Technology*, *59*(1), 16–33.
672 https://doi.org/10.1080/02786826.2024.2412999
673 Miao, R., Chen, Q., Zheng, Y., Cheng, X., Sun, Y., Palmer, P. I., Shrivastava, M., Guo, J., Zhang,
674 Q., Liu, Y., Tan, Z., Ma, X., Chen, S., Zeng, L., Lu, K., & Zhang, Y. (2020). Model bias in
675 simulating major chemical components of PM $_{2.5}$ in China. *Atmospheric Chemistry and*
676 *Physics*, *20*(20), 12265–12284. https://doi.org/10.5194/acp-20-12265-2020
677 Mitsakou, C., Housiadas, C., Eleftheriadis, K., Vratolis, S., Helmis, C., & Asimakopoulos, D.
678 (2007). Lung deposition of fine and ultrafine particles outdoors and indoors during a cooking
679 event and a no activity period. *Indoor Air*, *17*(2), 143–152. https://doi.org/10.1111/j.1600-
680 0668.2006.00464.x

Nenes, A., Pandis, S. N., & Pilinis, C. (1998). ISORROPIA: A New Thermodynamic Equilibrium Model for Multiphase Multicomponent Inorganic Aerosols. *Aquatic Geochemistry*, *4*(1), 123–152. https://doi.org/10.1023/A:1009604003981

Ng, N. L., Herndon, S. C., Trimborn, A., Canagaratna, M. R., Croteau, P. L., Onasch, T. B., Sueper, D., Worsnop, D. R., Zhang, Q., Sun, Y. L., & Jayne, J. T. (2011). An Aerosol Chemical Speciation Monitor (ACSM) for Routine Monitoring of the Composition and Mass Concentrations of Ambient Aerosol. *Aerosol Science and Technology*, *45*(7), 780–794. https://doi.org/10.1080/02786826.2011.560211

NOAA. (n.d.). *HYSPLIT – Air Resources Laboratory*. Retrieved January 11, 2025, from https://www.arl.noaa.gov/hysplit/

Paglione, M., Gilardoni, S., Rinaldi, M., Decesari, S., Zanca, N., Sandrini, S., Giulianelli, L., Bacco, D., Ferrari, S., Poluzzi, V., Scotto, F., Trentini, A., Poulain, L., Herrmann, H., Wiedensohler, A., Canonaco, F., Prévôt, A. S. H., Massoli, P., Carbone, C., … Fuzzi, S. (2020). The impact of biomass burning and aqueous-phase processing on air quality: a multi-year source apportionment study in the Po Valley, Italy. *Atmospheric Chemistry and Physics*, *20*(3), 1233–1254. https://doi.org/10.5194/acp-20-1233-2020

Salvador, P., Artíñano, B., Pio, C., Afonso, J., Legrand, M., Puxbaum, H., & Hammer, S. (2010). Evaluation of aerosol sources at European high altitude background sites with trajectory statistical methods. *Atmospheric Environment*, *44*(19), 2316–2329. https://doi.org/10.1016/j.atmosenv.2010.03.042

Salvador, P., Artíñano, B., Querol, X., & Alastuey, A. (2008). A combined analysis of backward trajectories and aerosol chemistry to characterise long-range transport episodes of particulate

matter: The Madrid air basin, a case study. *Science of The Total Environment*, *390*(2–3), 495–506. https://doi.org/10.1016/j.scitotenv.2007.10.052

Samoli, E., Atkinson, R. W., Analitis, A., Fuller, G. W., Green, D. C., Mudway, I., Anderson, H. R., & Kelly, F. J. (2016). Associations of short-term exposure to traffic-related air pollution with cardiovascular and respiratory hospital admissions in London, UK. *Occupational and Environmental Medicine*, *73*(5), 300–307. https://doi.org/10.1136/oemed-2015-103136

Shon, Z. H., Kang, M., Park, G., & Bae, M. (2020). Impact of temporary emission reduction from a large-scale coal-fired power plant on air quality. *Atmospheric Environment: X*, *5*, 100056. https://doi.org/10.1016/J.AEAOA.2019.100056

Stein, A. F., Draxler, R. R., Rolph, G. D., Stunder, B. J. B., Cohen, M. D., & Ngan, F. (2015). NOAA's HYSPLIT Atmospheric Transport and Dispersion Modeling System. *Bulletin of the American Meteorological Society*, *96*(12), 2059–2077. https://doi.org/10.1175/BAMS-D-14-00110.1

Stohl, A. (1996). Trajectory statistics-A new method to establish source-receptor relationships of air pollutants and its application to the transport of particulate sulfate in Europe. *Atmospheric Environment*, *30*(4), 579–587. https://doi.org/10.1016/1352-2310(95)00314-2

Stohl, A. (1998). Computation, accuracy and applications of trajectories—A review and bibliography. *Atmospheric Environment*, *32*(6), 947–966. https://doi.org/10.1016/S1352-2310(97)00457-3

Tobler, A. K., Skiba, A., Canonaco, F., Močnik, G., Rai, P., Chen, G., Bartyzel, J., Zimnoch, M., Styszko, K., Nęcki, J., Furger, M., Rózański, K., Baltensperger, U., Slowik, J. G., & Prevot, A. S. H. (2021). Characterization of non-refractory (NR) PM<inf>1</inf>and source

apportionment of organic aerosol in Kraków, Poland. *Atmospheric Chemistry and Physics*, *21*(19). https://doi.org/10.5194/acp-21-14893-2021

Vestreng, V., Myhre, G., Fagerli, H., Reis, S., & Tarrasón, L. (2007). Twenty-five years of continuous sulphur dioxide emission reduction in Europe. *Atmospheric Chemistry and Physics*, *7*(13), 3663–3681. https://doi.org/10.5194/acp-7-3663-2007

Wilks, D. S. (2019). Statistical Methods in the Atmospheric Sciences, Fourth Edition. In *Statistical Methods in the Atmospheric Sciences, Fourth Edition*. Elsevier. https://doi.org/10.1016/C2017-0-03921-6

Yarwood, G., Wilson, G., Emery, C., & Morris, R. (2024). User's Guide COMPREHENSIVE AIR QUALITY MODEL WITH EXTENSIONS. *Ramboll Environment and Health, Version 7.30*. www.ramboll.comwww.camx.comwww.camx.comwww.camx.comACKNOWLEDGMENTS

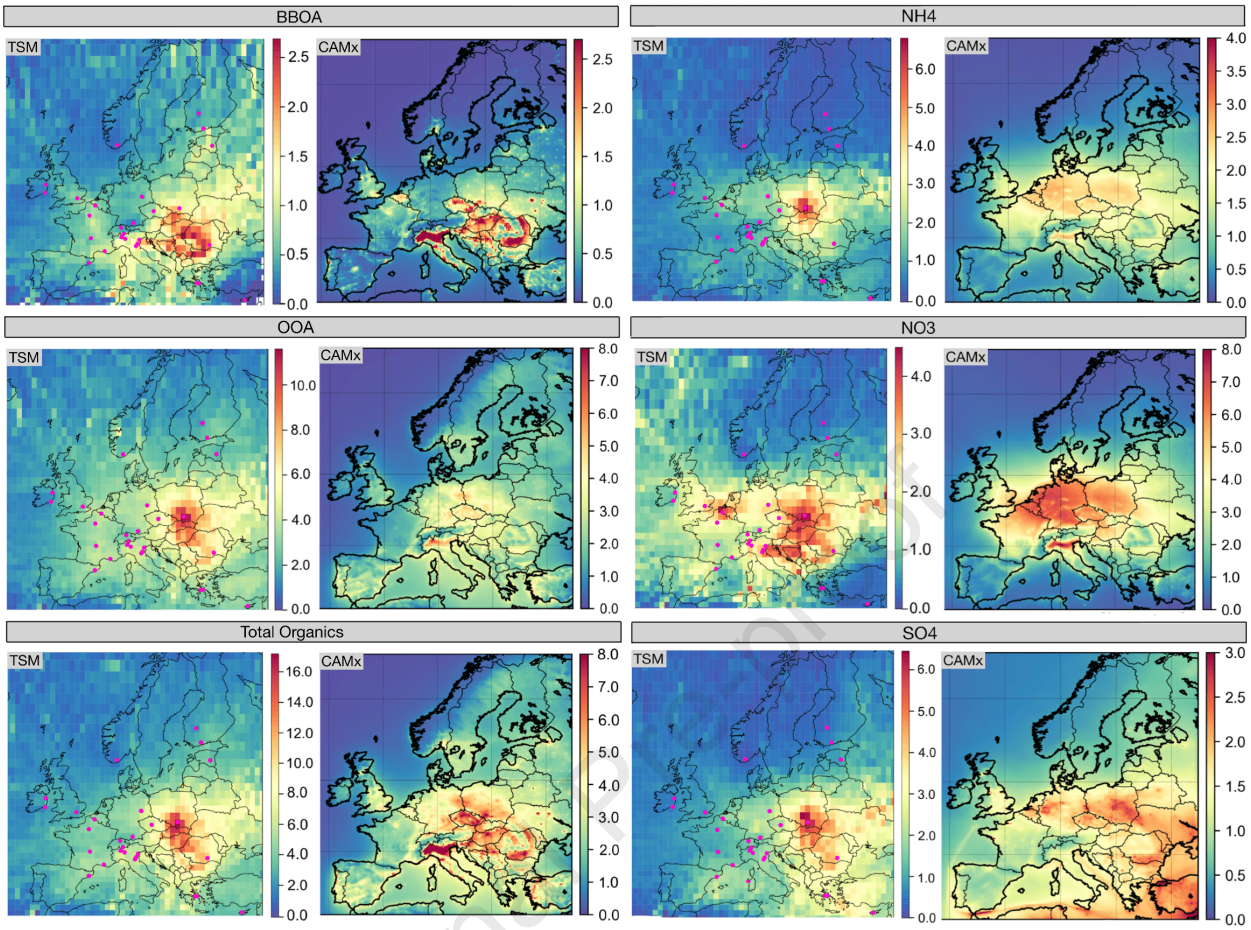

Highlights

- Long-range transport of PM species across Europe was analysed using 27 datasets;
- Concentrations of most PM components are highest in eastern Europe;
- TSM results aligned with CAMx output except for Po Valley and northern Europe;
- This study provides observation-based data to validate chemical transport models.

Declaration of interests

☒ The authors declare that they have no known competing financial interests or personal relationships that could have appeared to influence the work reported in this paper.

☐ The authors declare the following financial interests/personal relationships which may be considered as potential competing interests: